# Persistent Alterations in Dendrites, Spines, and Dynorphinergic Synapses in the Nucleus Accumbens Shell of Rats with Neuroleptic-Induced Dyskinesias

**Gloria E. Meredith,[1,4] Ian E. J. De Souza,[2,5] Thomas M. Hyde,[3] Geoffrey Tipper,[4] Mai Luen Wong,[4] and Michael F. Egan[3]**

*[1]Department of Basic Medical Science, University of Missouri-Kansas City, School of Medicine, Kansas City, Missouri 64108-2792, [2]Department of Zoology, Trinity College, University of Dublin, Dublin, Ireland, [3]Clinical Brain Disorders Branch, National Institute of Mental Health, Bethesda, Maryland 20892, [4]Department of Anatomy, Royal College of Surgeons in Ireland, Dublin 2, Ireland, and [5]Department of Biological Sciences, Open University, Milton Keynes, United Kingdom*

Chronic treatment of humans or experimental animals with classical neuroleptic drugs can lead to abnormal, tardive movements that persist long after the drugs are withdrawn. A role in these neuroleptic-induced dyskinesias may be played by a structural change in the shell of the nucleus accumbens where the opioid peptide dynorphin is upregulated in treated rats that show vacuous chewing movements (VCMs). The shell of the nucleus accumbens normally contains a dense plexus of dynorphinergic fibers especially in its caudomedial part. After 27 weeks of haloperidol administration and 18 weeks of withdrawal, the immunoreactive labeling of this plexus is intensified when compared with that after vehicle treatment. In addition, medium spiny neurons here show a significant increase in spine density, dendritic branching, and numbers of terminal segments. In the VCM-positive animals, the dendritic surface area is reduced, and dynorphin-positive terminals contact more spines and form more asymmetrical specializations than do those in animals without the syndrome (VCM-negative and vehicle-treated groups). Persistent, neuroleptic-induced oral dyskinesias could therefore be caused by incontrovertible alterations, involving terminal remodeling or sprouting, to the synaptic connectivity of the accumbal shell.

*Key words: tardive dyskinesia; vacuous chewing movement; D1 receptor; D2 receptor; odds ratio; opioid peptide*

Tardive dyskinesia (TD) developed by susceptible patients after chronic treatment with neuroleptic drugs can persist for years after the drugs are stopped. This disorder is slow to appear, and its pathophysiology is not well understood. Like humans, some rats treated long-term with haloperidol develop vacuous chewing movements (VCMs), a syndrome that mimics both the time course and symptoms of TD and thereby provides a good model of the disease (Egan et al., 1996; Hashimoto et al., 1998).

There is speculation that TD is caused by excitotoxicity (De Keyser, 1991). Extracellular glutamate is elevated, and glutamate transport is impaired in the striatum of long-term haloperidol-treated rats (Yamamoto and Cooperman, 1994; De Souza et al., 1999). Chronic neuroleptic treatment in rats is associated with increased perforations in dorsal striatal synapses, but decreased glutamate immunolabeling (Meshul and Tan, 1994; Meshul et al., 1996). The density and size of asymmetrical or symmetrical, dorsal striatal synapses are altered (Kerns et al., 1992; Roberts et al., 1995; Meshul et al., 1996; Mijnster et al., 1996), and spines or cells are reportedly lost from the dorsal striatum in VCM-positive (+) animals (Pakkenberg et al., 1973; Jeste et al., 1992; Kelley et al., 1997). Elevated levels of glutamate could cause all these changes. However, some data are conflicting, many alterations have been shown to occur independent of the abnormal movements, and most changes fail to persist after the drugs have been withdrawn.

In the nucleus accumbens in the ventral striatum, two territories, the core and shell, are differentially connected and regulated by dopamine (Deutch and Cameron, 1992; Zahm, 1992; Meredith et al., 1995). The shell has been proposed as a site of antipsychotic action (Deutch et al., 1992; Heimer et al., 1997), plays a role in feeding behavior and abnormal oral movements (Fletcher and Starr, 1987; Koshikawa et al., 1989; Deutch et al., 1992; Koene et al., 1993; Prinssen et al., 1994; Cools et al., 1995; Kelley and Swanson, 1997; Stratford and Kelley, 1997), but has yet to be linked to neuroleptic-induced structural change.

Endogenous opioid peptides, which are particularly sensitive to haloperidol treatment, are abundant in the ventral striatum (Meredith, 1999). Elevations in dynorphin mRNA in the accumbens have been associated with high VCMs (Egan et al., 1994, 1996). Dynorphin has also been linked to structural damage and motor dysfunction elsewhere (Long et al., 1988; Bakshi et al., 1990). Because the accumbal shell has a rich dynorphinergic network (Van Bockstaele et al., 1995), the question as to whether the dynorphin connections here are modified in TD becomes significant. The goal of these studies therefore was to examine, in a rat model of TD, how haloperidol affects the morphological structure of accumbal shell neurons and their dynorphinergic synaptic connections and whether structural changes persist in VCM+ rats after the drugs have been withdrawn.

Parts of this paper have been published previously (Meredith et al., 1997; De Souza et al., 2000).

## MATERIALS AND METHODS

Ninety-seven male Sprague Dawley or Wistar rats, weighing 150 gm at the start of the study, were housed two to a cage. Every 3 weeks for a period of 27 or 30 weeks, 71 animals were injected with 28.5 mg/kg haldol decanoate (equivalent of 1.0 mg/kg/day i.m.; McNeil Pharmaceuticals), and 26 were injected with vehicle (VEH; sesame oil). All rats were then kept for an additional 18–21 weeks during which they were given no further injections. The presence or absence of VCMs was monitored every 3 weeks before the injections. Rats were rated in a random order in an uncovered 20 × 30 × 40 cm plastic cage in front of a mirror. Each animal was unrestrained, and its vacuous chewing movements were counted for 2 min by a rater who was blind to the treatment. Two types of jaw move-

Received May 30, 2000; revised July 19, 2000; accepted July 27, 2000.

This research was supported by a grant from the Royal College of Surgeons in Ireland Research Committee and an equipment grant from the Health Research Board and the Wellcome Trust. We thank Drs. B. L. Roberts for helpful comments on this manuscript, J. Waddington for advice on the behavioral measures, S. Giles for technical assistance, and Ronan Conroy for his statistical help. The Media Services Department at the Royal College of Surgeons in Ireland gave valuable photographic assistance.

Correspondence should be addressed to Dr. G. E. Meredith, Department of Basic Medical Science, University of Missouri-Kansas City, School of Medicine, 2411 Holmes Road, Kansas City, MO 64108-2792. E-mail: email:meredithg@umkc.edu.

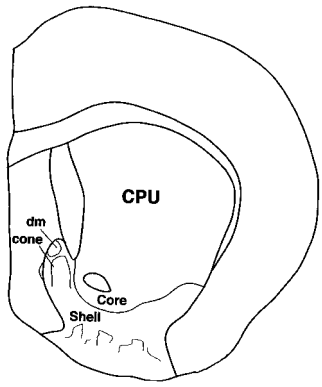


*Figure 1.* Diagram of a coronal section through the rat forebrain at a caudal level of the nucleus accumbens. Core and shell territories of the nucleus are labeled as are the dorsomedial (*dm*) and cone areas in the caudomedial shell. *CPU,* Caudate-putamen.

ments were observed: (1) an intermittent, isolated movement that was unrelated to grooming, gnawing, or mouthing food was counted as one movement, and (2) bursts of chewing, often associated with jaw tremors, usually consisted of two to six VCMs in rapid succession. The bursts were counted and analyzed separately but were not included in the data analysis. Tongue protrusions were observed and were also not counted. Scores were combined to assess the overall severity of the entire syndrome for each animal. Jaw movements were quantified over 14 rating sessions, and groups were compared. The 10 haloperidol-injected animals with the highest scores, and thus the most severe movements, during the final five rating periods constituted the VCM+ group. Twelve drug-treated animals with the least movements made up the VCM-negative (−) group. The remaining drug-treated animals were excluded from further analysis. Twelve VEH-treated animals were also selected at random for the study. Statistical comparisons were made between the selected groups (see Data analysis and statistics below).

After treatment and withdrawal periods, each animal was deeply anesthetized with a mixture of ketamine (70 mg/kg) and xylazine (6 mg/kg) intraperitoneally and perfused briefly with Tyrode's solution followed by fixative comprising 4.0% paraformaldehyde and 0.25% glutaraldehyde dissolved in 0.1 M phosphate buffer, if the brain tissue was to be used for ultrastructural study. Brains used for dendritic analyses were perfused with 3% paraformaldehyde and 15% saturated picric acid in 0.1 M phosphate buffer (Meredith et al., 1992). Ringer's and perfusion fluids were prepared as a single batch for all animals in each part of the study, and timings for administration of these fluids were kept uniform.

*Electron microscopic preparation.* After perfusion, each brain was removed and blocked, and the forebrain was cut into sections at 70 μm. Sections to be viewed with the electron microscope (EM) were submitted to a "freeze–thaw" regimen (Meredith and Arbuthnott, 1993) in which they were rinsed in an ascending series (5, 10, and 20%) of dimethylsulfoxide (DMSO) in phosphate (0.1 M) buffer, frozen in 20% DMSO solution, and allowed to defrost at room temperature.

All sections were pretreated overnight in 10% normal goat serum (NGS), rinsed, and incubated in rabbit anti-dynorphin A (Peninsula Laboratories), diluted 1:1000 in 0.05 M Tris-buffered saline with 1% NGS added, for 72 hr at 4°C, followed by incubation in biotinylated goat anti-rabbit IgG (1:200) for 9–12 hr at 4°C and in avidin–biotin complex for 6 hr at 4°C. Incubation media for light microscopic sections had 0.5% Triton X-100 added. Sections were reacted for 20 min in 0.05% 3,3′-diaminobenzidine tetrahydrochloride (DAB) with 0.01% $H_2O_2$, and, if prepared for light microscopy, were mounted on slides from a 0.2% gelatin solution, dehydrated, and coverslipped. Alternate sections, prepared for the EM, were treated with 1% osmium tetroxide in phosphate buffer for 30 min, dehydrated in ethanol, embedded in Epon resin, and allowed to polymerize for 48 hr at 60°C on glass slides. Uranyl acetate (1%) was added to the 70% alcohol step to increase contrast in the EM. All sections were then examined and photographed under the light microscope. Small blocks, cut from the cone area of the caudomedial shell of the nucleus accumbens (Fig. 1), were mounted with fresh Epon onto precured plastic blocks. Series of ultrathin sections were cut with a Reichert OM-U4 ultramicrotome, mounted on slot grids, contrasted with lead citrate, examined, and photographed in a Philips 301 EM. The immunostaining of tissue prepared for the EM was primarily superficial, because detergents were not used in the tissue preparation. Immunolabeled terminals were photographed at magnifications up to 70,000× and analyzed for a variety of features. Sections incubated without the primary antibodies showed no specific staining. The specificity of the primary antiserum has been tested previously by the use of immunoblots, and no significant cross-reactivity with enkephalin was found (Van Bockstaele et al., 1995).

Synaptic boutons were collected from 27 blocks prepared from the same location in the nucleus accumbens (Fig. 1) for equal numbers of rats in the three groups (three to five blocks per animal). Semiserial, ultrathin sections (~90 nm in thickness) were collected from each block and mounted onto grids. Because immunoreactive staining was very superficial, sections were only collected through the most superficial 2 μm of each block. Each ultrathin section was scanned thoroughly in the EM in the same manner, and all boutons that were immunoreactive and contained identifiable vesicles were photographed. A total of 5187 dynorphin-immunoreactive boutons (between 400 and 500 boutons per animal) were photographed initially. From these, only boutons that were considered to be synaptic (as decided independently by two investigators blind to the treatment) were accepted for analysis. Boutons were counted as synaptic when parallel, distinctly thickened, presynaptic and postsynaptic membranes were visible and separated by a narrow cleft, and there was a minimum of three vesicles in the immediate vicinity of the presynaptic membrane (Mijnster et al., 1996). If the postsynaptic membrane was at least three times the thickness of the presynaptic side, the synapse was considered asymmetrical. Synaptic thickenings that were discontinuous were judged to be perforated, even though serial sections were not analyzed. Synaptic targets were classified as somatic, if a clearly defined nucleus was present, or spinous, if a spine apparatus was visible. Small structures lacking a spine apparatus were identified as dendrites if their outer membrane was complete; synaptic targets that were too disrupted or too small to be identified were not included in the analysis. Bouton inclusions, dense core vesicles (DCVs), and puncta adhaerens were noted.

*Dendritic analysis.* Six VCM+, eight VCM−, and eight VEH-treated animals were used for this part of the study. Each brain was removed, and transverse slices 150 μm thick were cut (Fig. 1) and coded so that the investigator was blind to the animal's treatment at all times. Slices were counterstained with 4′,6-diamidino-2-phenylindole (DAPI) at a concentration of $10^{-7}$ M for 10 min to reveal neuronal somata. Each slice was viewed with a Nikon Optiphot 2UD microscope equipped with extra long working distance objectives and epifluorescence. A silver wire connected to a constant current source (Digitimer U.K.) was placed in a 4% aqueous solution of biotinylated Lucifer yellow (LY; Molecular Probes, Eugene, OR) in a glass pipette. The pipette was visually guided into each DAPI-stained perikaryon by the use of a motorized micromanipulator. A positive holding current of 1–5 nA was reversed after the pipette had impaled a cell, and LY was released with a negative current of 1–3 nA over a period of 10 min. Electrode resistance was maintained between 80 and 250 MΩ (cf. Meredith and Arbuthnott, 1993). After four to eight neurons were intracellularly filled with LY, the slice was incubated in an avidin–biotin complex for 90 min at room temperature and reacted with 0.05% DAB and 1% ammonium nickel sulfate added. Slices were then mounted onto glass slides from a 0.2% gelatin solution, dehydrated, and coverslipped.

Labeled neurons were analyzed only if they could be unambiguously assigned to the medial half of the shell of the nucleus accumbens and if their dendritic trees were well filled and the spines were visible. Morphometric analyses were performed by the use of a Nikon microscope and a motorized stage coupled to hardware and software (Neurolucida; Microbrightfield, Colchester, VT) dedicated to neuronal reconstruction. A Sholl analysis of ring intersections (Sholl, 1981) was used to estimate dendritic length. Spines were recorded with special markers, and spine density was expressed as the mean number of spines per 10 μm for all segments >50 μm in length (Meredith et al., 1995). The dendritic surface area was calculated by the use of the formula for the surface area of a frustum of a cone:

$$\text{Surface area} = \pi(R_1 + R_2)\sqrt{h2 + (R_1 - R_2)^2},$$

where $R_1$ is the radius at the start of that segment portion, $R_2$ is the radius at the end of that portion, and $h$ is the length. Branched and mushroom spines were also counted; the former had more than one head clearly connected to a common shaft (Comery et al., 1996; Robinson and Kolb, 1997), and the latter was so designated if the head was >0.3 μm in diameter.

*Data analysis and statistics.* Behavioral ratings were used to assess the effects of haloperidol treatment compared with VEH, the incidence of the VCM syndrome and its persistence in a subset of animals, and the effects of neuroleptic withdrawal on the VCM score. These data were analyzed with a repeated measures ANOVA with one between (groups of VCM+, VCM−, and VEH) and one within (time) factor. *Post hoc* comparisons of groups were conducted with Scheffe's *t* test.

The cross-sectional surface area and length of the active zones for all dynorphin-immunoreactive synaptic boutons were measured and expressed as a mean ± SEM. Values were pooled for respective animals of each group, and all groups were compared by the use of a one-way ANOVA. A Student's *t* test was used to compare two groups. The largest synaptic terminals (those >1 SD of the mean area) were compared separately by the use of ANOVA. Five synaptic variables were rated as present or absent: (1) asymmetrical synaptic specialization, (2) symmetrical synaptic specialization, (3) synaptic perforations of each active zone, (4) dynorphin immunoreactivity in the target, and (5) the structural nature of the synaptic target, i.e., spine, dendritic shaft, soma, or other. These variables could not be studied with simple parametric statistics or with unbiased stereology, because values were independent of volume and recorded simply as present or absent. All data summaries and statistical comparisons were performed blind to the treatment. We elected to analyze the data by the use of odds ratios (ORs), which predict the chances of an

event occurring when a set factor is present as compared with the odds of the event occurring in the absence of that factor. The Mann–Whitney *U* test was used to assess differences between groups, and unmatched univariate ORs were calculated on two subanalyses of the data. For these unmatched analyses, *p* values were calculated by the use of the two-tailed Fisher's Exact Test (for analyses with small numbers of observations); ORs (95% confidence intervals) were computed by using maximum likelihood procedures. Two comparisons of the values were made: (1) haloperidol treatment (VCM+ and VCM−) versus no treatment (VEH) and (2) abnormal movement (VCM+) versus no abnormal movement (VCM− and VEH).

To analyze dendritic and spine data, values were pooled for each group, and a Kolmogorov–Smirnov test was used to assess the normality of the distribution of each data set. Data sets not normally distributed were compared by the use of a Kruskal–Wallis ANOVA followed by *post hoc* nonparametric analysis with Mann–Whitney *U* tests. Normal data sets were compared by the use of ANOVA followed by *post hoc* Scheffe's tests or Student's *t* test, as appropriate. Comparisons were also made between groups with respect to dendritic branch order to ascertain the level of the dendritic branch where morphological parameters were altered.

## RESULTS

### Behavioral measures of vacuous chewing

Both Wistar and Sprague Dawley rats were used in this study. The behavioral data for these animals have been published previously (Egan et al., 1996; De Souza, 2000). Briefly, the results of these studies showed that over the 27–30 week treatment period, the haloperidol groups showed a gradual increase in VCMs compared with the VEH-treated group (treatment effect for Sprague Dawley rats, $F = 45.4$; df = 1; $p = 0.0001$; and for Wistar rats, $F = 9.378$; df = 1; $p = 0.0005$; treatment-by-time interaction for Sprague Dawley rats, $F = 3.7$; df = 13; $p = 0.0001$; and for Wistar rats, $F = 9.496$; df = 14; $p = 0.0001$).

When the VCM ratings were compared between groups, there was, as expected, a marked group effect for both strains ($p < 0.0007$). The ratings for the VCM+ rats of both strains slowly rose, because there was a group-by-time interaction ($p < 0.001$). Mean ratings of the VCM+ group during the last five sessions were significantly elevated compared with those of the vehicle and VCM− groups (Scheffe's *t* test, VCM+ vs VEH, $p = 0.0014$; and VCM+ vs VCM−, $p = 0.003$), whereas there was no difference between VCM− and VEH-treated groups for both strains. The VCM ratings did not differ between strains; ~40% of the animals showed significantly elevated VCMs throughout the treatment and withdrawal periods. However, the persistence of VCMs was not as pronounced during the withdrawal period for the Wistar strain as for the Sprague Dawley animals. In agreement with the work of Tamminga et al. (1990), VCM ratings for the high-VCM group of Wistar rats began to fall toward control values at the end of the withdrawal period, whereas that of the Sprague Dawley rats persisted at the same high level.

### Dynorphin immunoreactivity

At the light microscopic level, dynorphin immunostaining was heterogeneous in all animals, especially in the nucleus accumbens (Figs. 1, 2). It was seen primarily in varicose fibers and puncta, but also in some cell bodies lying within densely immunostained dynorphinergic plexuses (Fig. 2). At rostral levels, small areas enriched with dynorphin-immunoreactive fibers and varicosities were located dorsal and lateral to the anterior commissure (see also Van Bockstaele et al., 1994). Further caudal in the shell, densely immunoreactive zones were found medially, and in the core, small intensely immunoreactive zones were visible lateral to and above the anterior commissure (Fig. 2). Sections that were incubated without the primary antiserum showed no specific immunoreactive staining.

Distinctive differences between groups in the intensity, but not the pattern, of dynorphin immunoreactivity were discernible (Fig. 2). The greatest differences were found in the caudomedial shell, where the cone area (Fig. 1) enriched with dynorphin immunoreactivity was capped by a small, densely immunoreactive zone with a sharp border (dm; Figs. 1, 2, *insets*). The immunoreactive intensity gradually faded further ventrally in the shell. In the VCM+ rats, the borders of the cone and dm areas were more sharply

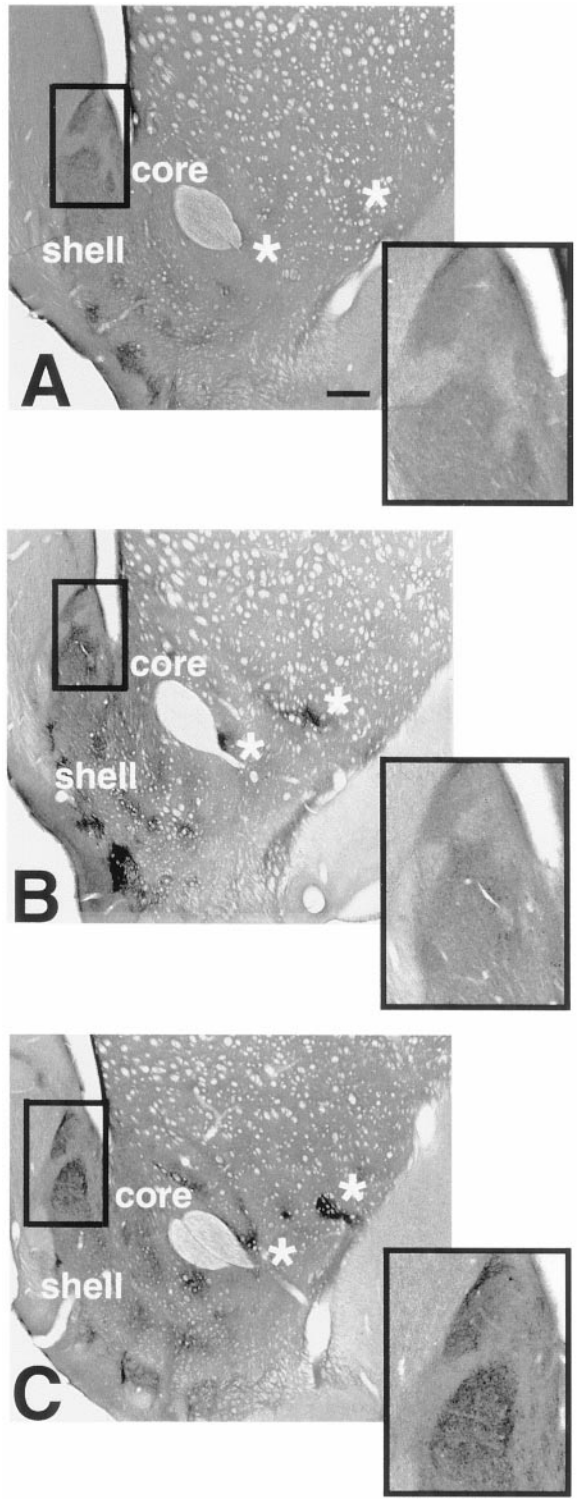


*Figure 2.* Light photomicrographs of sections through the neostriatum and caudal nucleus accumbens. Each section has been immunoreacted for dynorphin and is taken from a VEH-treated (*A*), VCM− (*B*), or VCM+ (*C*) rat. The caudomedial part of the shell of the nucleus accumbens (*boxed area*) has been enlarged in the *inset* of each micrograph. Note the intense immunoreactivity and sharp borders of the cone and dm (Fig. 1) areas of the shell in the VCM+ rat (*C*) as compared with those of the VCM− (*B*) and VEH-treated (*A*) animals. Note the homogeneous dynorphin immunoreactivity in the CPU. *Asterisks* mark small dynorphin-positive areas in the lateral core and shell of the nucleus. Note the increased immunoreactive intensity of these small regions in the VCM+ (*C*) rat as compared with that of the VCM− (*B*) and VEH-treated (*A*) animals. Scale bar: *A*, 500 μm (this scale bar is valid for *B* and *C*).

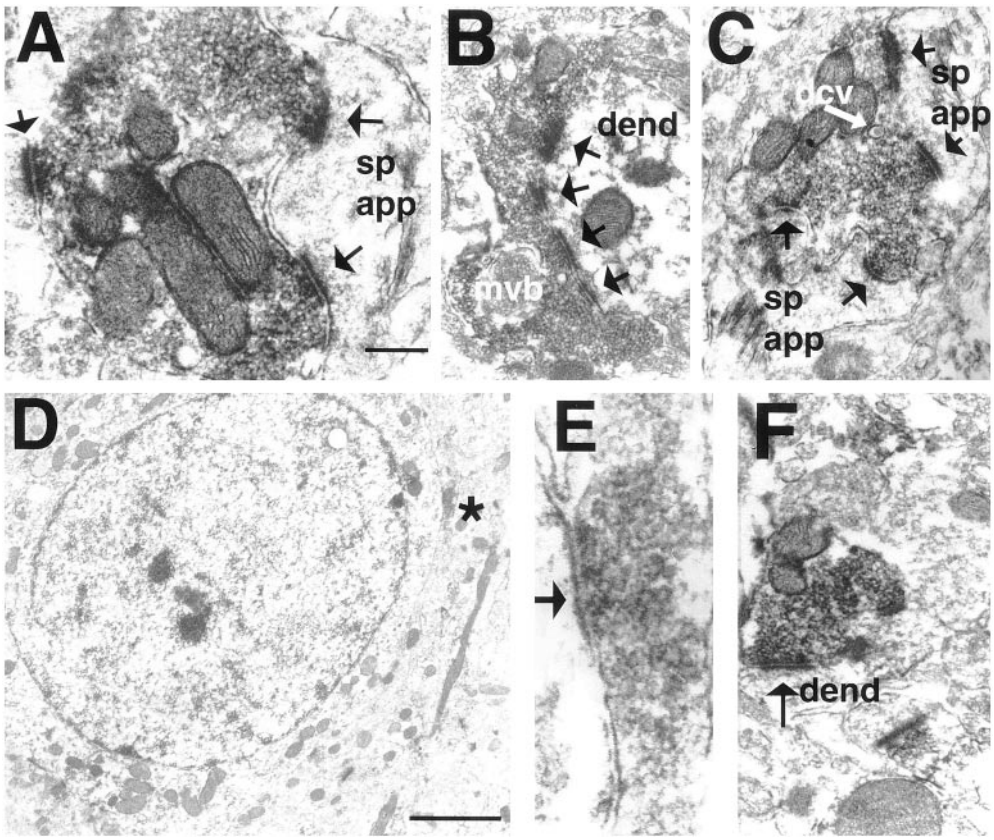


*Figure 3.* Electron micrographs taken from the shell of the nucleus accumbens in VCM+ (*A–C*), VCM− (*D, E*), and VEH-treated (*F*) rats. *A*, The dynorphin-immunoreactive terminal contacts two spines (*arrows* point to the active zone); one contact (*right side*) is perforated. *B*, A dynorphin-immunoreactive ending forms a perforated, asymmetrical synapse (4 perforations labeled with *arrows*) with a dendritic shaft (*dend*). Note the multivesicular body (*mvb*) within the terminal. *C*, A dense core vesicle (*dcv*) is marked with a *white arrow*. *D*, A dynorphin-positive terminal (*asterisk*) makes a symmetrical contact with the soma in a VCM− rat. Note the round, nonindented nuclear envelope, indicating that this is a medium spiny neuron. *E,* terminal seen in D (*asterisk*). *F,* A dynorphin-positive bouton makes a symmetrical synaptic contact with a dendritic shaft in a VEH-treated animal. Scale bars: *A*, 0.5 μm (valid for *B, C,* and *F*); *E,* 0.1 μm; *D,* 2 μm. *sp app,* spine apparatus.

delineated than were those seen in the other two groups of animals (Fig. 2, compare *C* with *A,B*). The cone (Fig. 1) was selected for ultrastructural analysis.

## Dynorphin-immunoreactive synapses

In the EM, dynorphin-immunoreactive axons and dendrites, but rarely somata, were found scattered in the tissue; immunolabeled terminals were also uncommon. All immunoreactive elements were characterized by the electron-dense DAB reaction product associated with vesicles (Fig. 3*A–C,E,F*). Nuclei of dynorphin-positive perikarya were never immunostained, and dynorphin-immunoreactive dendrites generally had spines. In total, 274 dynorphin-immunoreactive boutons were accepted as synaptic and were distributed in approximately equal numbers over the three groups. These synaptic terminals were filled with small clear vesicles (Fig. 3*F*) and primarily formed symmetrical contacts with dendrites (Fig. 3*B,F*) (see also Van Bockstaele et al., 1994, 1995). In the VCM− and VEH-treated groups, dynorphin-positive terminals occasionally contacted perikarya (Fig. 3*D,E*), the latter of which always had a round nuclear envelope characteristic of a medium spiny projection neuron (Fig. 3*D*). Dynorphin-immunoreactive terminals from all groups had other features in common, such as dense core vesicles (Fig. 3*C*), which were characteristically located away from terminal walls and the presynaptic specialization (Fig. 3*C*). Bouton inclusions and multivesicular bodies (Fig. 3*B*) were associated with 3–4% of all terminals; puncta adhaerens and vesicle-like, postsynaptic indentations were rare.

Most dynorphin-immunoreactive terminals formed a single synapse with one postsynaptic target (Fig. 3*B,E,F*). Nevertheless, 12% of the dynorphin-positive terminals in VEH-treated brains and 8% in VCM− brains made synaptic contacts with two or three postsyn-

**Table 1. Summary of dynorphinergic synaptic bouton features**

| Animal group | Mean bouton area ($\mu m^2$ ± SEM) | Mean active zone length (μm ± SEM) | Postsynaptic density | Perforated synapses | % Targets with dynorphin | Postsynaptic target | | |
|---|---|---|---|---|---|---|---|---|
| | | | | | | Spine | Dendritic shaft | Soma |
| VEH-treated | 0.53 ± 0.06 | 0.32 ± 0.02 | 84% symmetrical<br>16% asymmetrical | 8.2% | 30% | 3.6% | 76.8%‡‡ | 3.4% |
| VCM− | 0.40 ± 0.05 | 0.26 ± 0.01 | 82% symmetrical<br>18% asymmetrical | 4.6% | 41% | 6.3% | 77.1%‡‡ | 6.1% |
| VCM+ | 0.60 ± 0.05 | 0.31 ± 0.02 | 73% symmetrical*<br>27% asymmetrical** | 13.8% | 23%† | 29.8%‡ | 56.4% | 2.1% |

The cross-sectional terminal areas and active zone lengths were compared across groups (one-way ANOVA). Other synaptic variables were rated as present or absent for each group, and odds ratios were used to predict the chances of each variable being present (or absent) in VCM+ rats as compared with the odds of that feature occurring (or not occurring) in the absence of VCMs (VCM− and VEH-treated groups combined).

When compared with VEH-treated and VCM− animals, *dynorphin-immunolabeled terminals of VCM+ rats make significantly fewer symmetrical contacts ($p = 0.01$), **dynorphin-immunolabeled terminals of VCM+ rats are significantly more likely to end in an asymmetrical specialization ($p = 0.035$), †dynorphin-immunolabeled terminals in VCM+ rats contact significantly fewer dynorphin-positive targets ($p = 0.006$), and ‡dynorphin-immunolabeled terminals in VCM+ rats contact significantly more spines ($p = 0.003$).

When compared with VCM+ animals, ‡‡dynorphin-immunolabeled terminals in VCM− and VEH-treated rats contact significantly more dendritic shafts ($p = 0.003$).

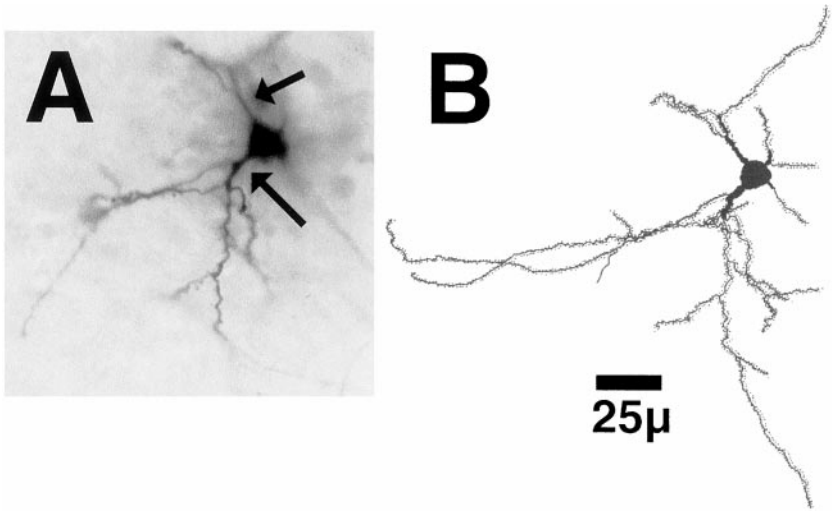


*Figure 4.* *A,* A typical neuron in the shell of the nucleus accumbens filled with biotinylated LY and reacted with DAB in a VEH-treated rat. Note the thickened, aspiny proximal dendritic segments (*arrows*). *B,* A reconstruction of the filled neuron pictured in *A*.

aptic targets; 21% of the terminals in VCM+ brains contacted more than one target (Fig. 3*A,C*). Furthermore, in the VCM+ material, 15% of the terminals that made multiple contacts formed more than three contacts.

The mean, cross-sectional area of dynorphin-immunoreactive terminals in the VCM+ group was 13% larger than that in VEH-treated rats (Table 1), but the difference was not significant. The largest (>1 SD above the mean) dynorphin-positive terminals were found in the VCM+ animals, but these were not significantly larger than those in the other two groups. Dynorphin-immunolabeled endings of the VCM+ animals were more likely to be perforated (Fig. 3*A,C*) and form multiple perforations (Fig. 3*B*) than were those in the other groups; however the difference was also not significant (Table 1). Dynorphin-positive boutons in VCM+ rats contacted significantly fewer dynorphin-positive targets [Table 1; odds ratio, 0.44; 95% confidence interval (0.3–0.7)], formed significantly more asymmetrical specializations [Table 1; odds ratio, 1.77; 95% confidence interval (0.3–0.9)], and contacted significantly more spines [Table 1; odds ratio, 5.79; 95% confidence interval (2.2–15.1)] and significantly fewer dendrites [$p = 0.02$; odds ratio, 0.55; confidence interval (1.1–2.9)]. Dynorphin-positive terminals contacted significantly more dendrites in the VCM− and VEH-treated groups than in the VCM+ group [Table 1; odds ratio, 2.61; 95% confidence interval (1.5–4.5)].

### Dendritic shafts and spines

Reconstructed neurons found in the caudomedial shell of VEH-treated rats showed the typical configuration (Fig. 4). They had three to six proximal dendritic segments, spine-free initial dendritic shafts, and densely spiny distal segments (Fig. 4*B*). Morphometric analyses showed significant differences in spine density, tortuosity, and dendritic shaft surface area and volume between groups (compare Figs. 5*A* with *B,C,* 6). There was a 25% increase in the spine density ($p < 0.01$) of neurons belonging to VCM+ and VCM− animals as compared with that of VEH-treated rats (Figs. 5, 6; Table 1). Spines also appeared on the proximal dendritic segments of VCM+ (Fig. 5*C*) and VCM− rats. There was, however, no change in the frequency of branched or mushroom-shaped spines for any of the groups (ANOVA; $F = 0.388$ and $p = 0.687$ for branched spines; $F = 1.906$ and $p = 0.195$ for mushroom-shaped spines).

Sholl (1981) analysis revealed a marked increase in branching, i.e., 47% more branch points ($p = 0.019$) and 36% more terminal segments ($p = 0.025$), in VCM+ and VCM− as compared with VEH-treated rats. The radial dendritic shaft length increased by 25.4% ($p = 0.058$), and neurons had more second (51%; $p = 0.030$)-, third (52%; $p = 0.047$)-, and fifth (234%; $p = 0.029$)-order dendritic segments for VCM+ and VCM− rats than for VEH-

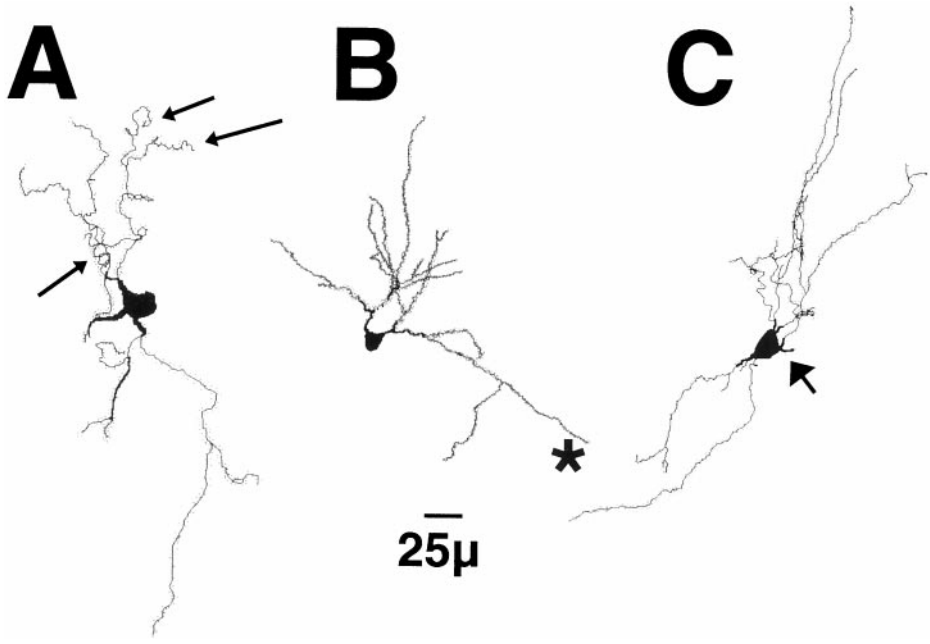


*Figure 5.* Reconstructions of typical, medium spiny neurons in the shell of the nucleus accumbens in a VEH-treated (*A*), VCM− (*B*), or VCM+ (*C*) rat. Note the tortuous distal dendritic segments (*small arrows*) in *A* and the straight segments in *B* (*asterisk*) and in *C*. Note the higher density of the spines in *B* and *C* as compared with that in *A* and the spines on the proximal dendritic segment (*large arrow*) in *C*.

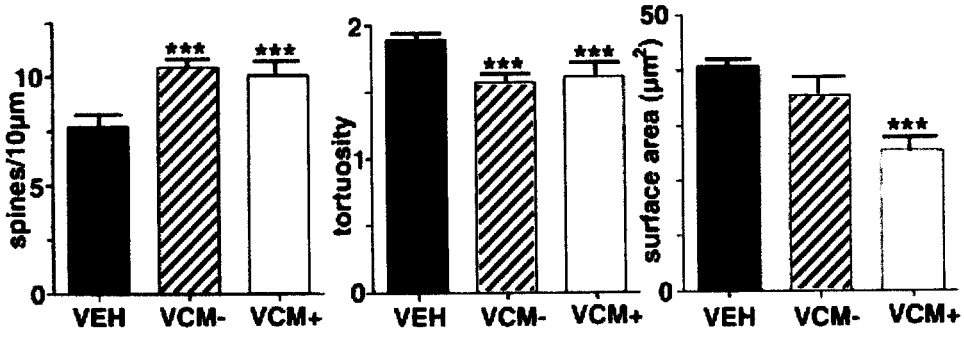


*Figure 6.* Bar graphs illustrate the significant differences between animal groups. Graphs show spine density (*left*), tortuosity (*middle*), and dendritic surface area (*right*) for VEH (*filled bar*), VCM− (*hatched bar*), and VCM+ (*open bar*) animals. The *left* and *middle* graphs show that spine density is significantly (*asterisks*) increased and tortuosity is significantly reduced for both VCM+ and VCM− groups. The *right* graph shows that dendritic segments in the VCM+ rats have significantly reduced surface areas as compared with those in the other two groups.

treated animals. Dendritic shafts of shell neurons in VEH-treated brains were significantly more tortuous than were those seen in VCM+ and VCM− material ($p < 0.01$; Figs. 5, 6). More importantly, in VCM+ rats, dendritic segments were decreased in surface area and volume (38% decrease; $p = 0.03$) when compared with those in VEH-treated controls (Fig. 6). There were no significant differences in dendritic volume or surface area between VCM− and VEH-treated rats (Fig. 6).

## DISCUSSION

These results show an unambiguous structural response by neurons in the shell of the nucleus accumbens to chronic haloperidol treatment. They further provide compelling evidence of dramatic and persistent changes in the dynorphinergic circuitry of the shell of the nucleus accumbens that are associated with neuroleptic-induced dyskinesia. The shifts in dynorphinergic synaptic contacts could be attributed to an increase in axodendritic contacts in VCM− and VEH-treated animals. However, it more likely involves the remodeling and/or sprouting of dynorphin-positive terminals in VCM+ rats (Fig. 7). Dynorphin mRNA is significantly upregulated (Egan et al., 1994), and medium spiny neurons are morphologically altered (present results) in the accumbal shell of these animals. These data provide clear evidence that a structural change in the dynorphinergic circuitry of the nucleus accumbens is associated with the movement syndrome (Fig. 7).

### Technical considerations

The intensity of dynorphin immunoreactivity in VCM+ rats was greater than that in other groups. Presumably this was not caused by false-positive labeling, because antibody specificity has been established (Pickel et al., 1993), but rather by an increase in the density of dynorphin-positive structures. Certainly, the light microscopic pattern of dynorphinergic elements did not differ between the three groups or from that in previous reports (Van Bockstaele et al., 1994). Furthermore, we controlled for variability in the fixation and immunocytochemical procedures (Mijnster et al., 1996). Another issue involves the use of odds ratios. Because there were multiple observations made on each experimental animal, the data could not be considered a simple random sample. Analyzing these data without taking this into consideration would have resulted in biased estimates of variance, leading to spuriously narrow confidence intervals. Therefore, the odds ratio allowed the best estimate of the relationship between the predictor variable and the outcome, and by adding the confidence intervals, effects that occur in a small data set could be tested (Altman et al., 1983; Gardner and Altman, 1986). Moreover, the morphological events that were compared by the use of these ratios did show clear increases or decreases in percentage terms.

### Long-term neuroleptic treatment is accompanied by synaptic modifications

Neuroleptic-induced oral dyskinesias are slow to develop both in experimental animals and humans and can persist indefinitely after cessation of drug treatment. Increased dopamine receptor binding has long been discarded as a responsible factor, and there is growing support for a structural basis (cf. Benes et al., 1985; Waddington, 1990; Mijnster et al., 1996). Ultrastructural studies have shown increases in the size and perforations of dorsal striatal synapses (Benes et al., 1985; Meshul and Casey, 1989; Roberts et al., 1995), but no change (Benes et al., 1985), a rise (Uranova et al., 1991; Kerns et al., 1992), or a decline (Roberts et al., 1995) in synaptic density in the caudate-putamen of chronically treated rats. Changes that have been reported consistently, such as increased perforations, seem to be specific for glutamatergic endings, and although these can be correlated with the development of VCMs (Meshul et al., 1994, 1996), they do not persist in VCM+ rats after drug withdrawal (Roberts et al., 1995). Certainly, drug dosage and the means of administration could be factors that influence these measures, but, more importantly, the synaptic parameters or the region selected may not be appropriate for the interpretation of the behavioral hypersensitivity.

### Why the shell of nucleus accumbens?

The structural changes described here are found in the caudomedial shell of the nucleus accumbens, a region densely innervated by dopaminergic fibers from the ventral tegmental area (Voorn et al., 1986; Brog et al., 1993). This part of the shell is contiguous with the extended amygdala and important for mediating not only neuroleptic drug actions but also the stress-induced sensitization of motor activity (Alheid and Heimer, 1988; Deutch and Cameron, 1992; Deutch et al., 1992; Kalivas et al., 1993). Shell circuits are involved in chewing, induced either by dopaminergic agents or during feeding behavior (Prinssen et al., 1994; Kelley and Swanson, 1997; Stratford and Kelley, 1997). The TD syndrome could therefore be attributed to this region, particularly because these abnormal oral movements are exacerbated during times of stress and anxiety (Tarsy, 1983).

The nucleus accumbens contains high levels of the dynorphin peptide and its related receptors (Meredith, 1999; Meshul and McGinty, 2000). The synthesis and release of this peptide are primarily regulated by activity at dopamine D1 receptors (Gerfen et al., 1990), which are rich in the shell of the nucleus accumbens (Bardo and Hammer, 1991). Chronic haloperidol treatment is accompanied by elevations in dynorphin mRNA in animals that develop tardive but not acute oral movements (Egan et al., 1996). The elevated dynorphin message may be in response to other changes brought about by haloperidol such as persistent endogenous dopamine release that increases activity at the D1 receptor or augmented levels of extracellular glutamate (Egan et al., 1991; See and Chapman, 1994). Certainly, κ receptor stimulation inhibits striatal glutamate release (Rawls and McGinty, 1998), suggesting that increased dynorphin production is an effort to compensate for elevated glutamate.

Patch-clamp recordings from acutely dissociated cells have shown that dynorphin reduces neuronal calcium currents and inhibits adenylate cyclase activity (Gross et al., 1990). In a series of experiments that examined immediate early gene induction by cocaine, Steiner and Gerfen (1998) concluded that dynorphin can inhibit dopamine release and blunt D1 receptor activation. This could occur via a negative feedback mechanism involving κ recep-

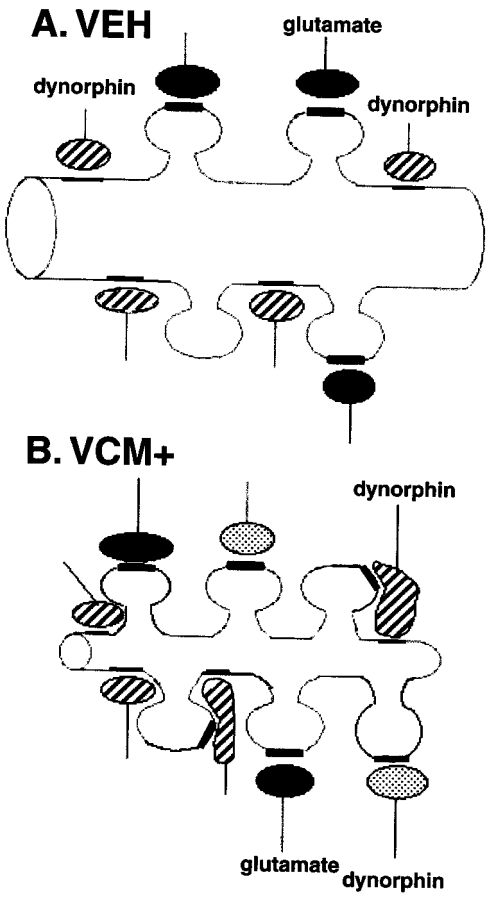


*Figure 7.* Schematic drawing of hypothetical changes that dynorphin-immunoreactive terminals undergo in animals that are VCM+. *A,* A sketch of a typical dendritic segment found in the shell of the nucleus accumbens of a VEH-treated rat. Dynorphin-positive endings (*hatched*) are shown contacting the dendritic shaft, and glutamatergic boutons (*filled*) are illustrated ending on spines. *B,* An illustration of a dendritic segment from a VCM+ rat. After 18 weeks of withdrawal from 27 weeks of haloperidol treatment, this dendrite has increased spine density and decreased surface area (see Fig. 6) when compared with that of the VEH-treated animal seen in *A*. In response to increased dynorphin production over the prolonged period, dynorphin-positive (*hatched*) axodendritic synapses change their shape and expand onto neighboring spines. Such growth would permit the receptor-bearing membrane located in the spine (Svingos et al., 1999) to come into close contact with a vesicle-bearing terminal, presumably rendering it functional. These dynorphinergic boutons would therefore form a new synapse on the spine, with the appropriate specialization, i.e., asymmetrical. Furthermore, new dynorphinergic terminals (*dotted*) may end on newly formed spines after axonal sprouting. Glutamate endings (*solid*) contact older spines. Regardless of the manner in which new synapses are formed, such structural modifications in dynorphin neurons and their synapses could alter the accumbal circuit in a dramatic and enduring manner.

tors located presynaptically on dopamine terminals (Svingos et al., 1999; Meshul and McGinty, 2000).

### Remodeling of shell circuits underlies the VCM syndrome

Dendritic surface area is an important parameter for synaptic arrangements, because the number of synapses that are present on a dendrite is proportional to the size of this feature (Harris and Kater, 1994). A decrease in surface area and the appearance of new spines would therefore have serious consequences for synapse stability (Halpain, 2000). Persistently elevated dynorphin (Egan et al., 1994) would ultimately require structural adaptations to accommodate the increase in peptide production. Some of our previous work has shown that subchronic haloperidol treatment alters the shape of striatal opioid synapses (Mijnster et al., 1996). Thus, increased dynorphin levels could lead to a change in the shape of existing terminals, which would allow boutons to maneuver onto newly formed spines and away from shrinking dendrites (Fig. 7). Because of these results, it is surprising therefore that dynorphinergic boutons were not significantly augmented in size in VCM+ rats. There could be technical reasons for this. Dynorphinergic terminals are uncommon, and serial sections were not collected because such an approach would have produced too few data points for statistical analysis. Therefore, the two-dimensional bouton areas recorded here may not have reflected the full size range of terminals in each group. Nevertheless, the tissue from VCM+ rats did contain the largest boutons and the greatest numbers of double or triple synapses of all the groups. Increased numbers of double synapses have been correlated with haloperidol-induced behavioral hypersensitivity (Kerns et al., 1992). The numbers of DCVs were also significantly increased for VCM+ rats as compared with those in other groups (data not shown). DCVs store peptides, and an increase in their numbers would signal a rise in dynorphin storage capacity (Van Bockstaele et al., 1994).

### Remodeling or sprouting of dynorphinergic terminals

New synapse formation or synaptogenesis is also likely for dynorphinergic endings (Fig. 7), even though total striatal synaptic density may decrease in VCM+ animals (Roberts et al., 1995). A new contact is not constrained in its synaptic specialization, and our results show that increases in asymmetrical specializations could reflect new synapse formation (Fig. 7), a possibility that has been proposed in synaptic turnover models (Dyson and Jones, 1984). Neither asymmetrical nor axospinous junctions are common for dynorphinergic endings (Van Bockstaele et al., 1994, 1995). There is evidence of haloperidol-induced sprouting in the substantia nigra (Benes et al., 1983), a region targeted mainly by dynorphinergic axons from the striatum. Moreover, synaptophysin, a ubiquitous glycoprotein associated with synaptic vesicles, is considered a direct measure of the presence of mature synapses, and an upregulation of this protein or its mRNA would indicate an increase in the absolute number of synapses (Marquèze-Pouey et al., 1991). Recently, we found a significant increase in synaptophysin mRNA after acute haloperidol administration in the accumbal shell (E. Hamid, G. Meredith, and M. Egan, unpublished observations), where axon collaterals of dynorphinergic neurons are common. Such an early elevation in synaptophysin message may be a first step in the sprouting process.

Significant reductions in the numbers of dynorphin-positive targets in VCM+ rats can possibly be explained by the fact that DAB deposits are not as obvious in spines as in other, larger structures (Pickel et al., 1988) or that reduced dendritic volume means less antigen present for immunolabeling. In early Huntington's disease, striatal dendrites become longer and thinner before cell death (Ferrante et al., 1991). It is possible that similar changes underlie the pathophysiology of this neuroleptic-induced motor disorder. Clearly further work is needed to elucidate the mechanisms fully.

## REFERENCES

Alheid GF, Heimer L (1988) New perspectives in basal forebrain organization of special relevance for neuropsychiatric disorders: the striatopallidal, amygdaloid and corticopetal components of the substantia innominata. Neuroscience 27:1–39.

Altman DG, Gore SM, Gardner MJ, Pocock SJ (1983) Statistical guidelines for contributors to medical journals. Br Med J 286:1489–1493.

Bakshi R, Newman AH, Faden AI (1990) Dynorphin A-(1–17) induces alterations in free fatty acids, excitatory amino acids, and motor function through an opiate-receptor-mediated mechanism. J Neurosci 10:3793–3800.

Bardo MT, Hammer Jr RP (1991) Autoradiographic localization of dopamine $D_1$ and $D_2$ receptors in the rat nucleus accumbens: resistance to differential rearing conditions. Neuroscience 45:281–290.

Benes FM, Paskevich PA, Domesick VB (1983) Haloperidol-induced plasticity of axon terminals in rat substantia nigra. Science 221:969–971.

Benes FM, Paskevich PA, Davidson J, Domesick VB (1985) The effects of haloperidol on synaptic patterns in the rat striatum. Brain Res 329:265–274.

Brog JS, Salyapongse A, Deutch AY, Zahm D (1993) The patterns of afferent innervation of the core and shell in the "accumbens" part of the

rat ventral striatum: immunohistochemical detection of retrogradely transported fluoro-gold. J Comp Neurol 338:255–278.
Comery TA, Stamoudis CX, Irwin SA, Greenough WT (1996) Increased density of multiple-head dendritic spines on medium-sized spiny neurons of the striatum in rats reared in a complex environment. Neurobiol Learn Mem 66:93–96.
Cools AR, Miwa Y, Koshikawa N (1995) Role of dopamine D1 and D2 receptors in the nucleus accumbens in jaw movements of rats: a critical role of the shell. Eur J Pharmacol 286:41–47.
De Keyser J (1991) Excitotoxic mechanisms may be involved in the pathophysiology of tardive dyskinesia. Clin Neuropharmacol 14:562–565.
De Souza IEJ (2000) Morphological change in nucleus accumbens as a basis for the development of haloperidol-induced movement disorders. PhD thesis, Trinity College, University of Dublin.
De Souza IEJ, McBean GJ, Meredith GE (1999) Chronic haloperidol treatment impairs glutamate transport in the rat striatum. Eur J Pharmacol 382:139–142.
De Souza IEJ, Dawson NM, Meredith GE (2000) Modification of dendritic morphology in nucleus accumbens' shell and core neurons following chronic haloperidol treatment as a basis for the development of vacuous chewing movements. Suppl Eur J Neurosci 12:135.
Deutch AY, Cameron DS (1992) Pharmacological characterization of dopamine systems in the nucleus accumbens core and shell. Neuroscience 46:49–56.
Deutch AY, Lee MC, Iadarola MJ (1992) Regionally specific effects of atypical antipsychotic drugs on striatal Fos expression: the nucleus accumbens shell as a locus of antipsychotic action. Mol Cell Neurosci 3:332–341.
Dyson SE, Jones DG (1984) Synaptic remodelling during development and maturation: junction differentiation and splitting as a mechanism for modifying connectivity. Brain Res 315:125–137.
Egan MF, Karoum F, Wyatt RJ (1991) Effects of acute and chronic clozapine and haloperidol administration on 3-methoxy-tyramine accumulation in rat prefrontal cortex, nucleus accumbens, and striatum. Eur J Pharmacol 199:191–199.
Egan MF, Hurd Y, Hyde TM, Weinberger DR, Wyatt RJ, Kleinman JE (1994) Alterations in mRNA levels of D2 receptors and neuropeptides in striatonigral and striatopallidal neurons of rats with neuroleptic-induced dyskinesias. Synapse 18:178–189.
Egan MF, Hurd Y, Ferguson J, Bachus SE, Hamid EH, Hyde TM (1996) Pharmacological and neurochemical differences between acute and tardive vacuous chewing movements induced by haloperidol. Psychopharmacology (Berl) 127:337–345.
Ferrante RJ, Kowall NW, Richardson EP (1991) Proliferative and degenerative changes in striatal spiny neurons in Huntington's disease: a combined study using the section-Golgi method and calbindin D28k immunocytochemistry. J Neurosci 11:3877–3887.
Fletcher GH, Starr MS (1987) Topography of dopamine behaviors mediated by D1 and D2 receptors revealed by intrastriatal injection of SJKF 38393, lisuride and apomorphine in rats with a unilateral 6-hydroxydopamine-induced lesion. Neuroscience 20:589–597.
Gardner MJ, Altman DG (1986) Confidence intervals rather than p values; estimation rather than hypothesis testing. Br Med J 292:746–759.
Gerfen CR, Engber TM, Mahan LC, Susel Z, Chase TN, Monsma Jr FJ, Sibley DR (1990) D1 and D2 dopamine receptor-regulated gene expression of striatonigral and striatopallidal neurons. Science 250:1429–1432.
Gross RA, Moises HC, Uhler MD, MacDonald RL (1990) Dynorphin A and cAMP-dependent protein kinase independently regulate neuronal calcium currents. Proc Natl Acad Sci USA 87:7025–7029.
Halpain S (2000) Actin and the agile spine: how and why do dendritic spines dance? Trends Neurosci 23:141–146.
Harris KM, Kater SB (1994) Dendritic spines: cellular specializations imparting both stability and flexibility to synaptic function. Annu Rev Neurosci 17:341–371.
Hashimoto T, Ross DE, Gao X-M, Medoff DR, Tamminga CA (1998) Mixture in the distribution of haloperidol-induced oral dyskinesias in the rat supports an animal model of tardive dyskinesia. Psychopharmacology (Berl) 137:107–112.
Heimer L, Harlan RE, Alheid GF, Garcia MM, De Olmos J (1997) Substantia innominata: a notion which impedes clinical-anatomical correlations in neuropsychiatric disorders. Neuroscience 76:957–1006.
Jeste DV, Lohr JB, Manley M (1992) Study of neuropathologic changes in the striatum following 4, 8 and 12 months of treatment with fluphenazine in rats. Psychopharmacology (Berl) 106:154–160.
Kalivas PW, Churchill L, Klitenick MA (1993) The circuitry mediating the translation of motivational stimuli into adaptive motor responses. In: Limbic motor circuits and neuropsychiatry (Kalivas PW, Barnes CD, eds), pp 193–236. Boca Raton, FL: CRC.
Kelley AE, Swanson CJ (1997) Feeding induced by blockade of AMPA and kainate receptors within the ventral striatum: a microinfusion mapping study. Behav Brain Res 89:107–113.
Kelley JJ, Gao XM, Tamminga CA, Roberts RC (1997) The effect of chronic haloperidol treatment on dendritic spines in the rat striatum. Exp Neurol 146:471–478.
Kerns JM, Sierens DK, Kao LC, Klawans HL, Carvey PM (1992) Synaptic plasticity in the rat striatum following chronic haloperidol treatment. Clin Neuropharmacol 15:488–500.
Koene P, Prinssen EP, Cools AR (1993) Involvement of the nucleus accumbens in oral behaviour in the freely moving rat. Eur J Pharmacol 233:151–156.
Koshikawa N, Aoki S, Hiruta M, Tomiyama K, Kobayashi M, Tsubio Y, Iwata K, Sumino R, Stephenson JD (1989) Effects of intrastriatal injections of selective dopamine D-1 and D-2 agonists and antagonists on jaw movements of rats. Eur J Pharmacol 163:227–236.
Long JB, Petras JM, Mobley WC, Holaday JW (1988) Neurological dysfunction after injection of dynorphin A-(1–13) in the rat. II. Non-opioid mechanisms mediate loss of motor, sensory and autonomic function. J Pharmacol Exp Ther 246:1167–1174.
Marquèze-Pouey B, Wisden W, Malosio ML, Betz H (1991) Differential expression of synaptophysin and synaptoporin mRNAs in the postnatal rat central nervous system. J Neurosci 11:3388–3397.
Meredith G, Egan MF, Tipper G, Wong ML, Hyde T (1997) Ultrastructural changes in dynorphinergic terminals of nucleus accumbens in rats that display neuroleptic-induced vacuous chewing movements. Soc Neurosci Abstr 23:399.
Meredith GE (1999) The synaptic framework for chemical signaling in nucleus accumbens. In: Advancing from the ventral striatum to the extended amygdala: implications for neuropsychiatry and drug abuse (McGinty J, ed), pp 140–156. New York: New York Academy of Sciences.
Meredith GE, Arbuthnott GW (1993) The challenge of *in vitro* preparations for morphological investigations. In: Morphological investigations of single neurons *in vitro* (Meredith GE, Arbuthnott GW, eds), pp 1–25. Chichester, UK: Wiley.
Meredith GE, Agolia R, Arts MPM, Groenewegen HJ, Zahm DS (1992) Morphological differences between projection neurons of the core and shell in the nucleus accumbens of the rat. Neuroscience 50:149–162.
Meredith GE, Ypma P, Zahm DS (1995) The effects of dopamine depletion on the morphology of medium spiny neurons in the shell and core of the rat nucleus accumbens. J Neurosci 15:3808–3820.
Meshul CK, Casey DE (1989) Regional, reversible ultrastructural changes in rat brain with chronic neuroleptic treatment. Brain Res 489:338–346.
Meshul CK, McGinty JF (2000) Kappa opioid receptor immunoreactivity in the nucleus accumbens and caudate-putamen is primarily associated with synaptic vesicles in axons. Neuroscience 96:91–99.
Meshul CK, Tan SE (1994) Haloperidol-induced morphological alterations are associated with changes in calcium/calmodulin kinase II activity and glutamate immunoreactivity. Synapse 18:205–217.
Meshul CK, Stallbaumer RK, Taylor B, Janowsky A (1994) Haloperidol-induced morphological changes in striatum are associated with glutamate synapses. Brain Res 648:181–195.
Meshul CK, Andreassen OA, Allen C, Jorgensen HA (1996) Correlation of vacuous chewing movements with morphological changes in rats following 1-year treatment with haloperidol. Psychopharmacology (Berl) 125:238–247.
Mijnster MJ, Ingham CA, Meredith GE, Docter GJ, Arbuthnott GW (1996) Morphological changes in met$^5$enkephalin-immunoreactive synaptic boutons in the rat neostriatum after haloperidol decanoate treatment. Eur J Neurosci 8:716–726.
Pakkenberg H, Fog R, Nilkanthan B (1973) The long-term effect of perphenazine enathate on the rat brain: some metabolic and anatomical observations. Psychopharmacologia 29:329–336.
Pickel VM, Towle AC, Joh TH, Chan J (1988) Gamma-aminobutyric acid in the medial rat nucleus accumbens: ultrastructural localization in neurons receiving monosynaptic input from catecholaminergic afferents. J Comp Neurol 272:1–14.
Pickel VM, Chan J, Sesack SR (1993) Cellular substrates for interactions between dynorphin terminals and dopamine dendrites in rat ventral tegmental area and substantia nigra. Brain Res 602:275–289.
Prinssen EPM, Balestra W, Bemelmans FFJ, Cools AR (1994) Evidence for a role of the shell of the nucleus accumbens in oral behaviour of freely moving rats. J Neurosci 14:1555–1562.
Rawls SM, McGinty JF (1998) κ-Receptor activation attenuates L-*trans*-pyrrolidine-2,4-dicarboxylic acid-evoked glutamate levels in the striatum. J Neurochem 70:626–634.
Roberts RC, Gaither LA, Gao X-M, Kashyap SM, Tamminga CA (1995) Ultrastructural correlates of haloperidol-induced oral dyskinesias in rat striatum. Synapse 20:234–243.
Robinson TE, Kolb B (1997) Persistent structural modifications in nucleus accumbens and prefrontal cortex neurons produced by previous experience with amphetamine. J Neurosci 17:8491–8497.
See RE, Chapman MA (1994) Chronic haloperidol, but not clozapine, produces altered oral movements and increased extracellular glutamate in rats. Eur J Pharmacol 263:269–276.
Sholl DA (1981) The organization of the cerebral cortex. London: Methuen.
Steiner H, Gerfen CR (1998) Role of dynorphin and enkephalin in the regulation of striatal output pathways and behavior. Exp Brain Res 123:60–76.
Stratford TR, Kelley AE (1997) GABA in the nucleus accumbens shell participates in the central regulation of feeding behavior. J Neurosci 17:4434–4440.
Svingos AL, Colago EEO, Pickel VM (1999) Cellular sites for dynorphin activation of κ-opioid receptors in the rat nucleus accumbens shell. J Neurosci 19:1804–1813.

Tamminga CA, Dale JM, Goodman I, Kaneda H, Kaneda N (1990) Neuroleptic-induced vacuous chewing movements as an animal model of tardive dyskinesia: a study in three rat strains. Psychopharmacology (Berl) 102:474–478.

Tarsy D (1983) Neuroleptic-induced extrapyramidal reactions: classification, description, and diagnosis. Clin Neuropharmacol 6:S9–S26.

Uranova NA, Orlovskaya DD, Apel K, Klintsova AJ, Haselhorst U, Schenk H (1991) Morphometric study of synaptic patterns in the rat caudate nucleus and hippocampus under haloperidol treatment. Synapse 7:253–259.

Van Bockstaele EJ, Sesack SR, Pickel VM (1994) Dynorphin-immunoreactive terminals in the rat nucleus accumbens: cellular sites for modulation of target neurons and interactions with catecholamine afferents. J Comp Neurol 341:1–15.

Van Bockstaele EJ, Gracy KN, Pickel VM (1995) Dynorphin-immunoreactive neurons in the rat nucleus accumbens: ultrastructure and synaptic input from terminals containing substance P and/or dynorphin. J Comp Neurol 351:117–133.

Voorn P, Jorritsma-Byham B, van Dijk C, Buijs RM (1986) The dopaminergic innervation of the ventral striatum in the rat: a light and electronmicroscopical study with antibodies against dopamine. J Comp Neurol 251:84–99.

Waddington JL (1990) Spontaneous orofacial movements induced in rodents by very long-term neuroleptic drug administration: phenomenology, pathophysiology and putative relationship to tardive dyskinesia. Psychopharmacology (Berl) 101:431–447.

Yamamoto BK, Cooperman MA (1994) Differential effects of chronic antipsychotic drug treatment on extracellular glutamate and dopamine concentrations. J Neurosci 14:4159–4166.

Zahm DS (1992) An electron microscopic morphometric comparison of tyrosine hydroxylase-immunoreactive innervation in the neostriatum and nucleus accumbens core and shell. Brain Res 575:751–756.